Proceedings of the 21st ICSMGE, Vienna, Austria, 14 – 19 June 2026. Pistrol, Adam & Schweiger (eds.)
Published by: ÖGG, Austrian Society for Geomechanics, Salzburg, Austria, ISBN 978-3-9503898-4-5
https://doi.org/10.53243/ICSMGE2026-713

Influence of floating diaphragm wall settlement on lateral earth pressure

Chu E. Ho
WSP USA, Chicago, Illinois, USA, chu.ho@wsp.com

ABSTRACT: This paper reviews the performance of floating diaphragm walls under vertical loading based on field observations of a cut-and-cover construction for an underground subway station in weak glacial silts. Vertical wall stability was provided mainly by sidewall shear resistance since the end bearing resistance was small, and the diaphragm wall must settle relative to the surrounding ground to mobilize sidewall resistance. Field monitoring indicated significant rotational wall deflections about the upper-level struts, accompanied by observable toe displacements and kick-back at the wall top. Measured lateral soil displacements behind the diaphragm walls suggest the active soil wedge developed close to the wall toes. Diaphragm wall settlements were estimated to range from 1.9 to 4.4 inches based on evaluation of ground loss and building settlements behind the diaphragm walls, implying significant yielding of the wall toes has taken place. Monitored strut loads showed that lateral earth pressures developed consistently exceeded the apparent earth pressure envelopes traditionally used for braced excavation design. The large lateral earth pressures were attributed to the reversal of the sidewall shear resistance, acting downwards on the active soil wedge, due to settlement of the diaphragm wall relative to the surrounding ground. It is proposed that excavation support loads for floating diaphragm walls be determined based on the combination of a modified Peck's apparent earth pressure envelope and the upper bound active earth pressure limit based on classical soil mechanics, assuming an active earth pressure coefficient (K_a) corresponding to Coulomb's theory which accounts for the direction of sidewall shear resistance.

KEYWORDS: Floating diaphragm wall, vertical loading, wall deflection, wall settlement, strut load, lateral earth pressure.

1 INTRODUCTION

Conventional design of embedded retaining walls for deep braced excavations often considers only the lateral stability of the excavation support system and requires wall toe embedment in a competent soil stratum or rock primarily for lateral restraint against toe kick-out. It is commonly assumed that the active soil wedge will displace downwards relative to a vertically unyielding wall, which will induce sidewall shear that resists sliding of the soil wedge and results in reduced lateral active earth pressures behind the wall.

However, under normal construction conditions, embedded retaining walls in braced excavations will also be subjected to vertical loads to a certain degree. Vertical loads can arise from dead and live loads from temporary bracings (or permanent slabs in top-down construction), or inclined anchor forces in addition to the self-weight of the wall itself and any loads acting at the top of the wall. As excavation and support installation are often implemented in sequential stages, increasing magnitude of vertical loads will be imposed on the retaining wall as the excavation progresses. Ingram et al. (2009) discussed the behavior of embedded retaining walls subjected to vertical loading. The authors highlight the necessity for vertical load equilibrium to be maintained in addition to consideration of lateral stability. The most critical condition will occur at the final excavation stage, prior to casting of the structural base slab, when the embedded length of the wall below the excavation subgrade is shortest and vertical loading will be largest.

In cases where the competent soil stratum or rock is deep, and it is uneconomical to extend the retaining wall to reach them, the retaining wall will be required to be designed as a floating foundation embedded in weak soils. Settlement of the retaining wall must then take place relative to the surrounding ground to mobilize upward sidewall shear resistance to maintain vertical wall stability since the end bearing component will be small. Simultaneously, this sidewall shear will act as a downward drag force on the active soil wedge behind the wall. Based on Coulomb's theory, this reversal of sidewall shear acting on the active soil wedge will increase the active earth pressure behind the wall (Coulomb, 1776).

This paper investigates the influence of floating diaphragm wall settlement on lateral earth pressures based on field observations of a cut-and-cover subway station construction in Manhattan, New York.

2 CASE STUDY

2.1 *Project Background*

The Metropolitan Transportation Authority's Second Avenue Subway Phase 1 extension project in New York City was completed and opened to the public in December 2016. The project provided a link from the existing 63rd Street Station at Lexington Avenue to an existing tunnel at 99th Street along Second Avenue on the east side of Manhattan Island. The 96th Street Station involved a cut-and-cover excavation approximately 60 ft wide and up to 70 ft deep, stretching from 92nd Street at the south end to 99th Street at the north end (Figure 1). The ground conditions varied significantly, from shallow rock between 92nd Street and 93rd Street to progressively deeper rock with increasing thickness of soft soils north of 93rd Street. Various aspects of the design and construction of the 96th Street Station have been previously discussed by Ho and Hu (2014), Grigson et al. (2016) and Ho (2022, 2024).

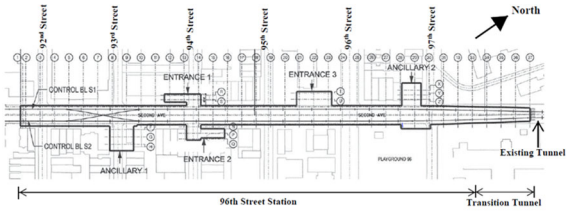

Figure 1. Cut-and-cover construction at 96th Street Station.

2.2 *Ground Conditions*

The subsurface soil stratification at the soft ground zone comprised of fill, organics, silty sands and glacial silts. The thickness of fill was highly variable, ranging from 10 to 30 feet across the site. The fill consisted of a complex composition of very loose to loose fine to medium sand and silt, with some clayey silt, and mixed with traces of gravel and brick fragments. The lower levels of the fill close to the interface with the organics layer were often infiltrated with soft silty clay with traces of roots. The organics layer was about 5 to 20 feet thick,

and it generally consisted of soft organic silt or silty clay with traces of peat, shells or fine sand and was classified as highly plastic. The silty sand stratum was about 5 to 30 feet thick, composed mainly of loose to medium dense fine sands with non-plastic silt. The glacial deposit extended below the silty sand to depths beyond 120 feet, comprising loose non-plastic silts with some fine sand, and laminated with thin seams of clayey silt, silty clay or very fine sand varves. Groundwater table was approximately 10 feet below ground. Table 1 summarizes the design parameters for the soils encountered.

Table 1. Geotechnical design parameters

Soil Strata	Unit Weight (pcf)	Undrained Shear Strength (psf)	Friction Angle (deg)	Cohesion (psf)
Fill	120	-	30	0
Organics	110	$0.325\sigma'_{vo}$	25	0
Silty Sand	120	-	33	0
Glacial Silt	125	-	32	0

Continuous cone penetration test (CPT) measurements taken through the soil layers indicated no increase in the cone tip resistance for the glacial silts (average $Q_t = 80$ tsf) to at least 100 feet below ground surface (Figure 2).

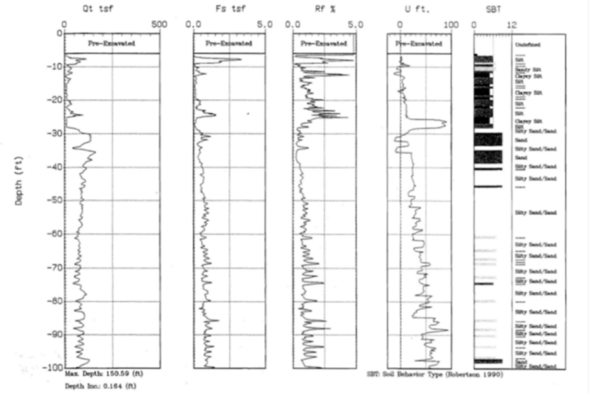

Figure 2. CPT profile in soft ground.

2.3 *Excavation Support Scheme*

Various excavation support systems were implemented in the project. Primarily, excavation support in shallow rock consisted of temporary secant pile walls installed with toes socketed into hard rock for groundwater cutoff, and the subway station box was constructed within the excavation seated on the rock. Where the rock was deep and excavation was carried out entirely in soft ground, 3.5 feet thick structural diaphragm walls were installed for excavation support. The diaphragm walls also formed the permanent station walls and were integrally connected to the station invert, platform and roof slabs. Between 93rd Street and 94th Street the diaphragm wall toes terminated in rock or decomposed rock. Beyond 94th Street, the diaphragm walls were completely floated in the soft ground, terminating within the glacial silts.

Figure 3 shows the typical floating diaphragm wall scheme adopted in the soft ground zone. During construction, a temporary steel traffic deck was erected spanning across the top of the diaphragm walls on each side of the excavation and lateral support was provided by two to three levels of steel pipe struts below the deck. The diaphragm walls were installed up to 100 feet deep. An embedment length of 40 feet beneath the final excavation subgrade was required for a typical 60 feet deep excavation for basal stability control within the glacial silts. Additionally, the diaphragm walls were required to support vertical loads imposed by the traffic deck and utilities hung from it, including self-weight of the struts/walers and diaphragm walls.

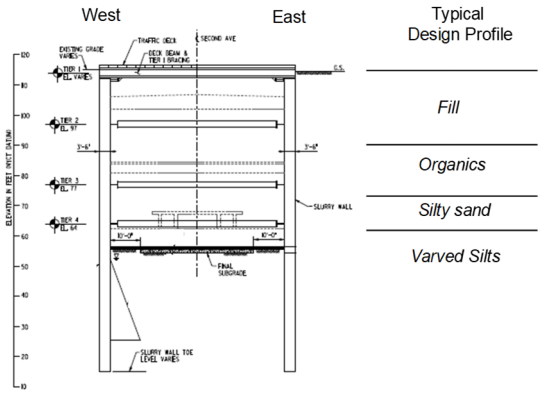

Figure 3. Typical floating diaphragm wall and lateral support scheme.

3 FIELD OBSERVATIONS

3.1 *Diaphragm Wall Deflections*

Figure 4 shows the lateral displacement profiles indicated by inclinometers installed within floating diaphragm walls. The excavation at inclinometer INW-95-3 was supported by two pipe struts (T2 and T3) below the traffic deck, whereas the excavations at inclinometers INW-95-2 and INW-95-4 were supported by three pipe struts (T2, T3 and T4) below the traffic deck. As can be seen, large wall deflections were observed with maximum values ranging from 1.7 to 2.0 inches and corresponding lateral toe displacements of 1.2 to 1.4 inches. A kick-back of up to 0.7 inches was observed in the upper part of the diaphragm walls. The significant kick-back at the wall top indicated the upper deck beam was free to slide and no significant axial compression forces will develop in the deck girder beam.

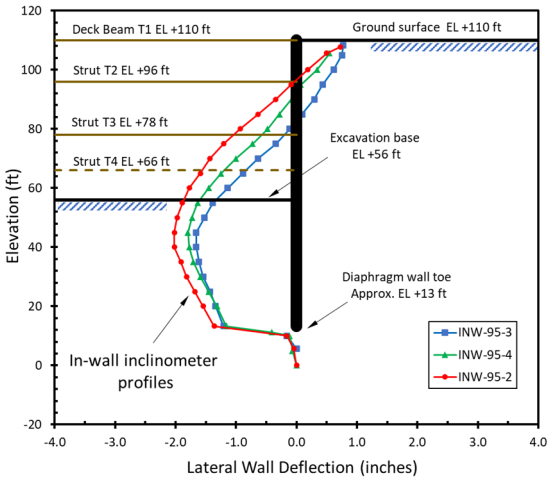

Figure 4. Lateral diaphragm wall deflections.

It was noted that all three in-wall inclinometer profiles indicated an abrupt transition at the wall toe. The very small deformations (< 0.16 inches) observed in the underlying soil suggested deep-seated plastic yielding had not occurred below the wall toe. The large translational failure mode at the wall toe could be attributed to the characteristic low resistance of the varved

glacial silt laminations in the horizontal direction (Ladd and DeGroot 2003, Parsons 1976). It also suggests large active earth pressures were induced close to the toe of the wall.

Figure 5 shows the displacements of the soil at in-soil inclinometers located approximately 5 feet behind the diaphragm walls. As can be seen, the abrupt transition between the concave and convex shape of the soil displacement curves indicated the rupture surface in the soil developed approximately 10 feet above the adjacent diaphragm wall toe at the inclinometer positions. This confirmed the active sliding failure plane extended close to the diaphragm wall toe.

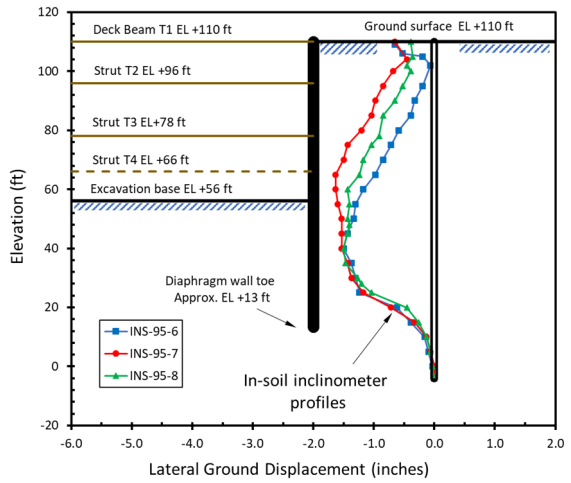

Figure 5. Lateral soil displacements behind diaphragm wall.

3.2 *Apparent Earth Pressures*

The loads developed in selected pipe struts were monitored using vibrating-wire strain gage measurements. The lateral support pressures derived from the maximum observed strut loads at three locations (S29, S48 and S41 strut series) are shown in Figures 6 to 8 for an excavation depth, H_e = 54 feet. The maximum strut loads included all sequences of strut installation and removal stages. It was assumed the structural steel girder for the traffic deck does not contribute to lateral support of the diaphragm walls due to the observed kick-back at the wall top, therefore all lateral loads were deemed to be resisted by the pipe struts below it.

Strut series S29 and S48 consisted of two struts below the traffic deck and the observed loading pattern in the struts were very similar, with the lower-level struts registering significantly larger loads than the upper-level struts. Three struts were installed at S41 below the traffic deck. Here, the loading pattern indicated the loads in the upper two struts were more evenly distributed, although the lowest strut still registered significantly larger loads than the two upper-level struts.

The characteristics of the ground behind the diaphragm walls were dominated by granular fill, silty sand and glacial silt, which were generally free draining. The apparent earth pressure envelopes proposed by Peck (1969) and Tschebotarioff (1973) for cohesionless soils are shown in Figures 6 to 8 for comparison. Peck (1969) considered a uniform coefficient of lateral earth pressure, K = 0.65 K_a for the full depth of excavation, where K_a is Rankine's active earth pressure coefficient for smooth walls (Rankine, 1857),

$$K_a = tan^2(45 - ½\emptyset') \quad (1)$$

Tschebotarioff (1973) assumed K increases linearly from zero at the ground surface and excavation base to the maximum value of 0.25 at $0.1H_e$ below the ground surface and $0.2H_e$ above the excavation base respectively.

An average unit weight of γ = 120 pcf, and friction angle of ϕ' = 30° (giving K_a = 0.33) were assumed in determining the earth pressure envelopes.

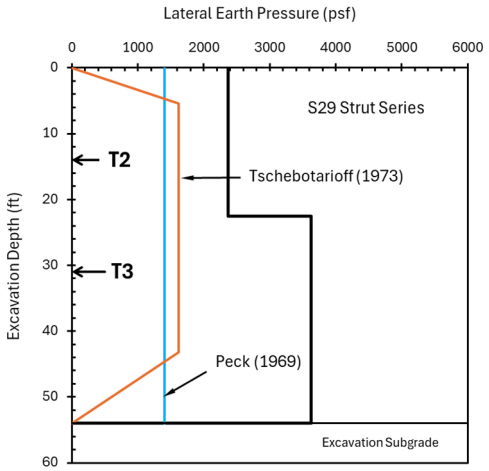

Figure 6. Lateral support pressures and traditional earth pressure envelopes (S29 Strut Series).

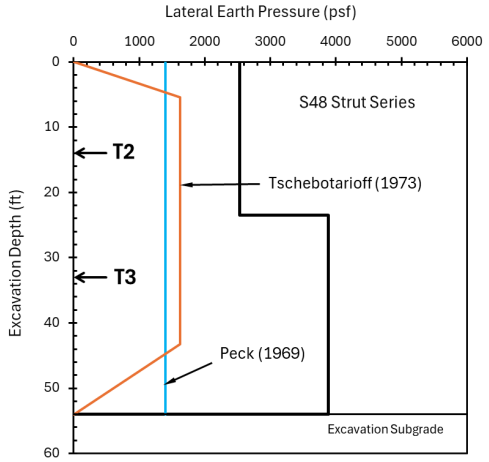

Figure 7. Lateral support pressures and traditional earth pressure envelopes (S48 Strut Series).

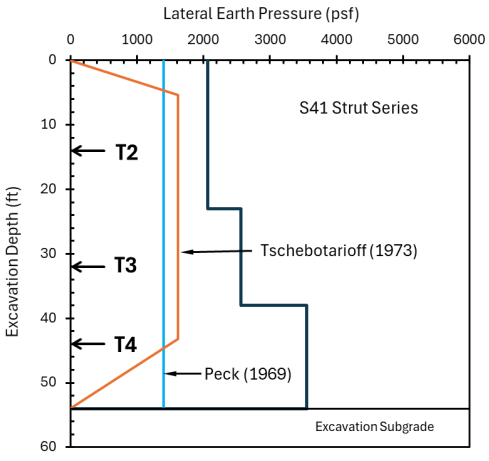

Figure 8. Lateral support pressures and traditional earth pressure envelopes (S41 Strut Series).

As can be seen, the actual support pressures exceeded the apparent earth pressure envelopes proposed by Peck (1969) and Tschebotarioff (1973) in all three cases.

3.3 *Diaphragm Wall Settlement*

The unique feature of a floating diaphragm wall scheme is the fact that settlement of the wall must take place relative to the adjacent ground to mobilize sidewall shear resistance for vertical stability. In this project, it was not possible to monitor the settlement at the top of the diaphragm wall directly since the traffic deck was seated on it. Ho (2024) demonstrated that it was possible to estimate the settlement of the diaphragm wall assuming the ground settlement profile behind the diaphragm wall follows a parabolic relationship as proposed by Bowles (1996), with the maximum ground settlement occurring at the diaphragm wall face (Figures 9 and 10). The volume of ground loss behind the diaphragm wall was assumed to be equal to the volume of lateral wall deflection based on Peck (1969).

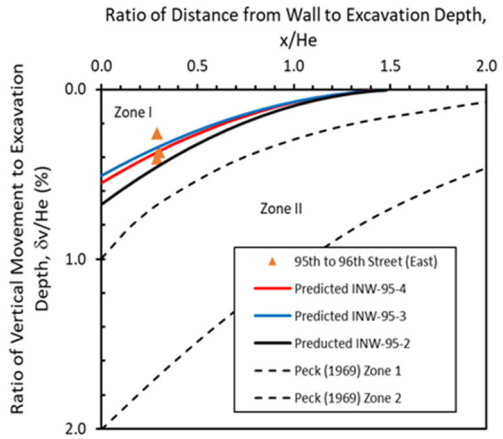

Figure 9. Ground settlement profiles between 95th and 96th Street.

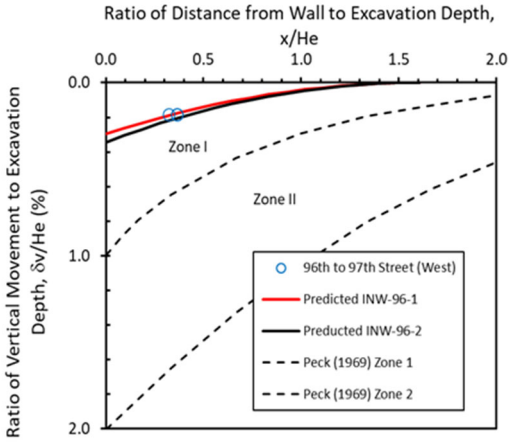

Figure 10. Ground settlement profiles between 96th and 97th Street.

It has been previously shown that small to medium-sized structures with unreinforced masonry load-bearing walls, such as for this project, do not possess sufficient rigidity to alter the ground movements induced by excavations (Boscardin and Cording 1989, Boone et al. 1999, Boone and Westland 2004). Therefore, the observed building settlements based on survey measurements can be used as a check on the ground profiles obtained. As can be seen from Figures 9 and 10, the derived ground settlement profiles based on in-wall inclinometer measurements (designated INW) correlated well with observed settlements of building facades facing the excavation (shown as triangular and circular data points).

The inferred maximum settlements at the floating diaphragm wall faces ($x/H_e = 0$) ranged from 0.51% to 0.68% of the excavation depth, H_e = 54 feet (or δ_v = 3.3 to 4.4 inches) for the East wall between 95th Street and 96th Street, and 0.29% to 0.34% of H_e (or δ_v = 1.9 to 2.2 inches) for the West wall between 96th Street and 97th Street. These wall settlements amounted to 4.5% to 10.5% of the diaphragm wall thickness (B = 3.5 feet) which was indicative of the behavior of a foundation element with significant yielding occurring at the wall toe under vertical compression loading.

4 INFLUENCE OF WALL SETTLEMENT ON LATERAL EARTH PRESSURE

Figure 11 shows the comparison of loads acting on the active and passive soil wedges for a conventional unyielding diaphragm wall founded in competent soil and a vertically yielding floating diaphragm wall founded in weak soils. The key difference is the direction of the sidewall shear transmitted to the active soil wedge, which will influence the magnitude of lateral earth pressure behind the wall. The direction of sidewall shear action on the passive soil wedge remains unchanged in both cases.

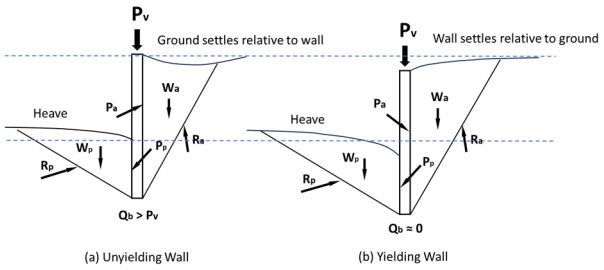

Figure 11. Forces on soil wedges for unyielding and yielding walls.

A parametric study was performed to investigate the influence of diaphragm wall settlements on the development of lateral earth pressures using Equation (2) based on classical soil mechanics theory proposed by Coulomb (1776), which accounts for the direction of soil-wall interface friction angle (δ) acting at the active soil wedge behind the wall.

$$K_a = \frac{sin^2(\alpha+\phi')}{sin^2(\alpha)sin(\alpha-\delta)\left\{1+\sqrt{\frac{\sin(\phi'+\delta)\sin(\phi'-\beta)}{\sin(\alpha-\delta)\sin(\alpha+\beta)}}\right\}^2} \quad (2)$$

where α, β and δ are defined as shown in Figure 12a.

In Figure 12a, W_s is the self-weight of the active soil wedge, R_a is the resistance along the rupture surface and P_a is the active earth load inclined at an angle which depends on the soil-wall interface friction angle (δ). For the present study, α = 90 degrees, β = 0, and ϕ' = 30° are assumed. Figure 12b depicts the active soil condition corresponding to the conventional assumption of upward acting sidewall shear (+δ) for an unyielding diaphragm wall. Figure 12c illustrates the condition of a downward sidewall shear (-δ) due to settlement of a yielding diaphragm wall.

The horizontal and vertical components of the active earth load (P_{ah} and P_{av}) are given by Equations (3a) and (3b).

$$P_{ah} = P_a \cos\delta \quad (3a)$$

$$P_{av} = P_a \sin\delta \quad (3b)$$

P_{ah} represents the earth load resisted by horizontal struts and P_{av} is equal to the sidewall shear resistance.

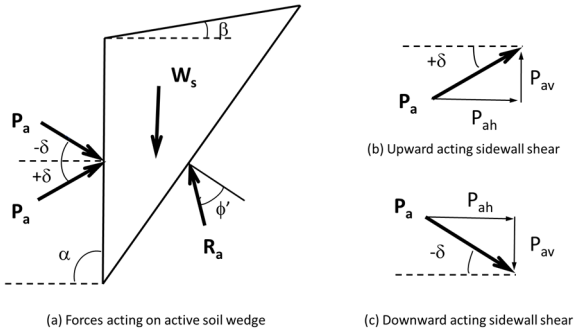

Figure 12. Forces on active soil wedge and directions of soil-wall interface friction angle (δ).

Figures 13 to 15 present the horizontal components of the Coulomb active earth pressures ($K_{ah} = K_a \cos\delta$) at the final excavation stage in terms of total lateral stress (summation of effective lateral soil stress and water pressure) in comparison with the lateral support pressures inferred from maximum measured strut loads. The upper and lower bound limits correspond to soil-wall interface friction angle ranging between $-\phi' < \delta < \phi'$ assuming the diaphragm wall face to be rough. The hydrostatic water pressure, U_w and at-rest earth pressure, $K_o = 1 - \sin\phi'$ (Jaky, 1944) are also included for reference. As can be seen, the downward acting sidewall shear on the active soil wedge could potentially increase the lateral earth pressure for a conventional non-yielding diaphragm wall condition ($\delta = \phi'$and $K_{ah} = 0.26$) to the upper bound value corresponding to a yielding diaphragm wall condition ($\delta = -\phi'$ and $K_{ah} = 0.75$), which may even exceed the at-rest earth pressure ($K_o = 0.5$).

It is well established that active earth pressure profiles based on classical soil mechanics theory tend to underestimate loads in upper-level struts in braced excavations due to soil arching within the soil wedge behind the wall (Lambe and Whitman, 1969). It is proposed in this paper that Coulomb's upper bound active earth pressure limit be adopted in combination with a modified Peck's apparent earth pressure envelope assuming $K = 0.65K_{ah}$ where K_{ah} is based on Coulomb's theory for $\delta = -\phi'$ (Figures 13 to 15).

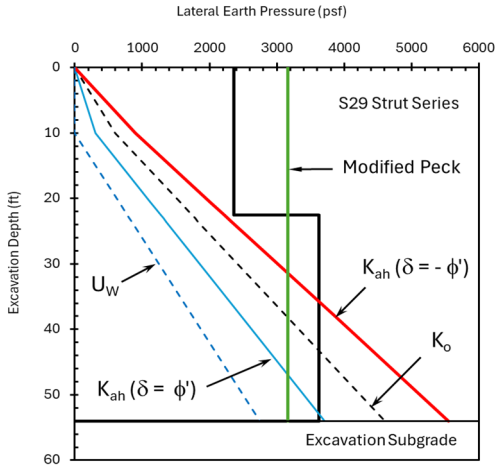

Figure 13. Lateral earth pressure profiles for S29 Strut Series.

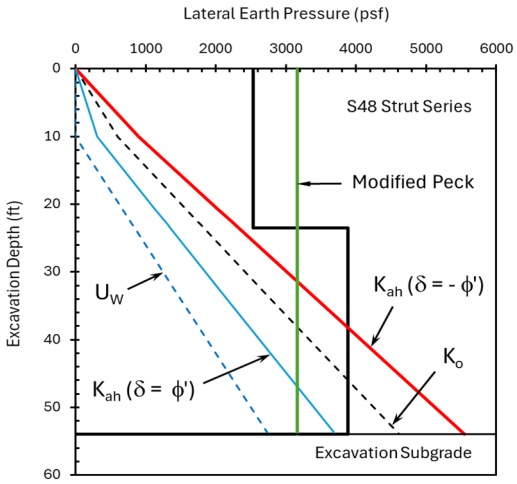

Figure 14. Lateral earth pressure profiles for S48 Strut Series.

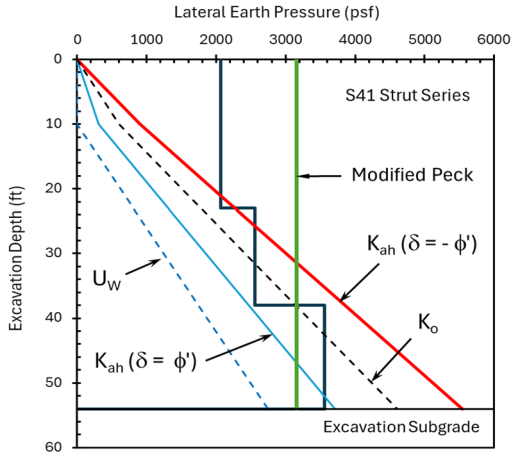

Figure 15. Lateral earth pressure profiles for S41 Strut Series.

Table 2 compares the maximum measured strut loads against the values calculated using Coulomb's upper bound active earth pressure limit and the modified Peck's apparent earth pressure envelope.

Table 2. Measured and estimated strut loads

Strut Series	Strut Level	Measured Load (ton)	Coulomb Upper Bound* (ton)	Modified Peck* (ton)
S29	T2	479.3	216.0 (2.22)	639.7 (0.75)
	T3	1028.1	1100.9 (0.93)	895.6 (1.15)
S48	T2	536.0	236.5 (2.27)	668.1 (0.80)
	T3	1067.7	1080.4 (0.99)	867.1 (1.23)
S41	T2	451.2	238.7 (1.89)	690.2 (0.65)
	T3	364.9	436.7 (0.84)	450.2 (0.81)
	T4	540.5	714.6 (0.76)	480.2 (1.13)

*Bracketed values represent the ratio of measured to calculated loads

As can be seen, values derived based on Coulomb's upper bound active earth pressure limit predicted reasonably well the loads for the lower-level struts (T3 and T4), but grossly underpredicted the loads for the upper-level struts (T2) by a factor of approximately two in all cases. Conversely, the modified Peck envelope gave results that were adequate for the upper-level struts (T2) in all cases, but underpredicted the

lowest struts (T3 in S29 and S48, and T4 in S41). The results for the middle strut (T3) in S41 were comparable in magnitude using both methods and were greater than the measured strut load.

The above study suggests that traditional apparent earth pressure envelopes using Rankine's value for K_a (Equation 1) may not be adequate for design of braced excavations involving floating diaphragm walls in weak soil conditions. An adjustment to the envelopes is necessary based on a value of K_a that reflects the development of higher active earth pressures due to settlement of the diaphragm wall relative to the surrounding ground. Additionally, strut loads should be checked against Coulomb's upper bound active earth pressure limit considering full reversal of the sidewall shear on the active soil wedge in order to account for higher loads developed in lower-level struts. The governing design load should be taken as the larger of the two calculated values for each strut.

By extension, where numerical modeling is used for analyzing braced excavation problems, it is recommended that the model should include appropriate vertical loads imposed on diaphragm walls to ensure that the influence of wall settlement on lateral earth pressure is properly accounted for in the design of excavation support elements.

5 CONCLUSIONS

This paper presents an investigation into the influence of floating diaphragm wall settlement on lateral earth pressures based on field observations of a cut-and-cover construction of an underground subway station in Manhattan, New York. Due to the large depth of competent soil or rock, the diaphragm walls were terminated in weak glacial silt deposits. Vertical loading was imposed on the diaphragm walls by a temporary traffic deck that spanned between the tops of the diaphragm walls with utilities hanging from it, including two to three levels of steel pipe struts and self-weight of the diaphragm walls. Vertical load resistance was provided mainly by sidewall shear resistance, with little contribution from end bearing resistance in the weak glacial silts.

Significant lateral wall deflections of 1.7 to 2.0 inches were observed with rotational wall movements about the upper-level struts and kick-back up to 0.7 inches at the wall top. Large translational displacements of 1.2 to 1.4 inches occurred at the wall toes indicating significant active earth pressures were developed near the wall toe. This was confirmed by in-soil inclinometers installed adjacent to the back of the wall which indicated the active rupture surface likely extended close to the wall toe. Estimated diaphragm wall settlements ranged from 1.9 to 4.4 inches, indicating a yielding wall condition.

Back-analysis of monitored strut loads indicated that lateral support pressures were much greater than for a conventional retaining wall that typically terminates in a competent soil layer. The observed pattern of lateral wall deflections and the significant settlement of the diaphragm walls suggest the large lateral earth pressures likely resulted from a reversal of the side-wall shear resistance when the floating diaphragm walls settled relative to the surrounding ground under the imposed vertical loading.

Traditional earth pressure envelopes based on Peck (1969) or Tschebotarioff (1973) may not be adequate for design of braced excavations involving floating diaphragm walls. Adjustment to the envelopes may need to be made, using an active earth pressure coefficient (K_a) that reflects the development of higher active earth pressures due to settlement of the diaphragm wall relative to the surrounding ground. Additionally, strut loads should be checked against Coulomb's upper bound active earth pressure limit assuming full reversal of the sidewall shear on the active soil wedge. The governing design load should be taken as the larger of the two calculated values for each strut.

Where numerical modeling is used for analyzing braced excavation problems, it is recommended that the model should include appropriate vertical loads imposed on diaphragm walls to ensure that the influence of wall settlement on lateral earth pressure is properly accounted for in the design of excavation support elements.

6 REFERENCES

Boone, S.J. and Westland, J. 2004. Design, construction and performance of a deep braced excavation. *Proc. 5th International Conference on Case Histories in Geotechnical Engineering*, New York, NY, Paper 5.57.

Boone, S.J., Westland, J., and Nusink, R. 1999. Comparative evaluation of building responses to an adjacent braced excavation. *Canadian Geotechnical Journal*, NRC, 36, 210-223.

Boscardin, M.D. and Cording, E.J. 1989. Building response to excavation-induced settlement. *Journal of Geotechnical Engineering*, ASCE, 115 (1), 1-21.

Bowles, J.E. 1996. *Foundation Analysis and Design*, 5th Edition, McGraw-Hill, New York.

Coulomb, C.A. 1776. Essai sur une application des regles de maximis et minimis a quelques problemes de statique relatifs a l'architecture. *Memoires de la Mathematique et de Phisique,* l'Academie Royale de Science, L'Imprimerie Royale, Paris, France, Vol.7, 343-382.

Grigson, R., Ho, C. and LeMus, P. 2016. Second avenue subway project: deep excavation support of a cut-and-cover station. *Proc. Geotechnical and Structural Engineering Congress 2016*, Phoenix, AZ, Chandran C. Y. and Holt M. I. eds., ASCE, 402-415.

Ho, C.E. 2022. Control of seepage pressures beneath cut-and-cover excavation in varved glacial silt. *Geotechnical Special Publication* No.332, ASCE, 529-543.

Ho, C.E. 2024. Ground loss behind floating diaphragm walls in soft ground excavation. *Geotechnical Special Publication* No.361, ASCE, 410-423.

Ho, C.E., and Hu, S. 2014. Design optimization of underground subway station diaphragm walls using numerical modeling, *Geotechnical Special Publication* No.234, ASCE, 3122-3132.

Ingram, P.J., Chodorowski, A.R., Anderson, S.E., and Gaba,, A.R. 2009. Design methodology for retaining walls for deep excavations in London using pseudo finite element methods. *Proc. 17th International Conference on Soil Mechanics and Geotechnical Engineering*, Alexandria, Egypt, IOS Press, 1437-1440.

Ladd, C.C., and DeGroot, D.J. 2003. Recommended practice for soft ground site characterization: Arthur Casagrande Lecture. *Proc. 12th Panamerican Conference on Soil Mechanics and Geotechnical Engineering*, MIT, Cambridge, MA, USA.

Lambe, T.W. and Whitman, R.V. 1969. *Soil Mechanics*, John Wiley and Sons Inc., New York.

Jaky, J. 1944. The coefficient of earth pressure at rest." *Journal of the Society of Hungarian Architects and Engineers,* Vol. 7, 355-358.

Parsons, J.D. 1976. New York's glacial lake formation of varved silt and clay. *Journal of Geotechnical Engineering Division*, ASCE, Vol. 102, No. GT6, 605-638.

Peck, R.B. 1969. Deep excavations and tunneling in soft ground. *Proc. 7th International Conference on Soil Mechanics and Foundation Engineering*, Mexico City, State-of the Art, 225-290.

Rankine, W.J.M. (1857). "On the stability of loose earth." *Philosophical Transactions of the Royal Society of London*, England, Vol.147, 9-27.

Tschebotarioff, G.P. 1973. *Foundations, Retaining Walls and Earth Structures*. McGraw-Hill Book Co., New York , 642 pp.